3-D Simulation of T-Shaped Electrode and Comparison of Results with Experiments

Yeong Kyo Shin[a*], Tae Su Hwang[a], Seok Dong Kang[a*], Hun Gun Park[a*], Jae Hwa Ryu[a*], Hyun Chul Kim[b], Seung Won Shin[b], and Jae Koo Lee[b]

Abstract

Numerical simulation is one of the most useful tools to study gas discharge phenomena that occur in alternating current plasma display panel (AC-PDP) cell. Most PDP cell simulations have been performed for two-dimensional cell, is cross-section along the address electrode. We developed a three-dimensional PDP simulator and applied it to a T-shaped electrode cell in order to show the effects of sustain electrode shape that cannot be included in two-dimensional simulation. The dependence of power consumption on electrode shape and area in the simulation showed the same trend as experiment.

Keywords : plasma display panel, gas discharge, numerical simulation

1. Introduction

Alternating current plasma display panel (AC-PDP) is the most promising candidate in the large flat display market. Now, there are companies the its mass production. But there still remain some problems that must be solved, such as the low luminance efficiency. One of the methods for increasing luminance efficiency is decreasing power consumption. Reducing power consumption is an important issue especially in high resolution displays such as XGA class and in large size exceeding 50 inch. When the area of sustain electrode is reduced, the consumed power can also be reduced. The T-shaped electrode of Pioneer Electronic Corp. [1] is a representative model for reducing sustain electrode area.

Because of the micro-size cell dimension, there are not many diagnostic tools for investigating directly inside the cell. Numerical simulation has been a useful tool for understanding discharge phenomena in the cell. But most PDP simulations [2,3] are based on two-dimensional (2-D) analysis along the address electrode. Although the 2-D simulation gives good guide lines for design factors such as ITO width, gas, gap size, thickness of dielectric, etc., it does not cover the effect of sustain electrode shape. Recently, the variations of electrode shape have been studied [4,5] so as to increase luminance efficiency. Thus we have developed a three-dimensional fluid simulator to model PDP cell and applied it to T-shaped sustain electrode structure [6,7].

Manuscript received February 6, 2002; accepted for publication March 22, 2002.

* Member, KIDS.
Corresponding Author : Yeong Kyo Shin
a. Digital PDP Division, LG Electronics Inc. 191-1 Kongdan-dong, Gumi-city Kyungsang Buk-do, 730-030, Korea.
b. Pohang University of Science and Technology San 31 Hyoja-Dong, Nam-Gu, Pohang Kyungsang Buk-do, 790-784, Korea.
E-mail : shinyk@lge.com **Tel** : +54 460-7380 **Fax** : +54 460-7323

2. Simulation Model and Conditions

Our model is based on the solution of transport equations (continuity equations and momentum transfer equations in drift-diffusion approximation) for particles and Poisson equation for the electric field [2]. The semi-implicit coupling of the Poisson equation and the

continuity equation makes it possible to increase the simulation time step over the dielectric relaxation time [8]. Implicit scheme solving continuity equation also makes it possible to overcome CFL time restriction. By using this code, we can understand the effects of three-dimensional parameters, such as shape of electrodes, barrier ribs, and the width of the address electrode, which cannot be included in the usual two-dimensional simulations.

The cell size is 810 × 270 μm^2 with 120 μm barrier rib height. The gap between the scan and sustain electrode is 60 μm. Ne-Xe(6 %) 500 torr gas mixture is used. Applied voltage frequency is 100 KHz with duty ratio 30 %. Voltage pulses have 100nsec rising and falling time. The address voltage is half the sustain voltage.

Simulation results are obtained in steady state. Alternating pulses are applied to sustain electrodes after the cell ignition between the scan and address electrodes. In this simulation, straight barrier rib is considered even although it is actually slant. 43 × 39 × 19 grids are considered in our simulation.

The discharge efficiency ρ producing UV photons can be defined by the ratio

$$\rho = \frac{P_{uv}}{P_{Discharge}}$$

where P_{uv} is the energy used in producing UV photons and $P_{Discharge}$ is energy dissipated in the discharge, i.e, energy used in heating electrons and ions during the discharge pulse [3].

3. Results

Fig. 1 shows the effects of barrier rib and address electrode width. The existence of barrier ribs is one of the big differences between 2-D and 3-D simulation results. Because the discharge region is smaller due to barrier ribs and the loss of plasma density toward barrier ribs brings about a decrease in the accumulated charge on the upper dielectric layer, plasma density becomes the smaller in the case with barrier ribs. Fig. 1(b) shows the potential difference (ΔV_y) between the upper dielectric layer and the lower dielectric layer at z=90 μm which is right outside the address electrode in the case of address electrode of 70 μm in width. In the case of an address electrode of 150 μm in width, the cross section at z=90 μm passes through the address electrode. In the case of 150 μm address electrode the width has higher potential difference than that of 70 μm address electrode width. Because the potential difference (ΔV_x) between the sustain electrodes is nearly the same for the two cases when the address electrode width is increased, the ratio ΔV_x of ΔV_y is decreased. Thus, the more plasma densities are obtained in the case of the smaller address electrode width. In the case of barrier ribs, when address electrode width is increased over 150 μm, electron densities become saturated.

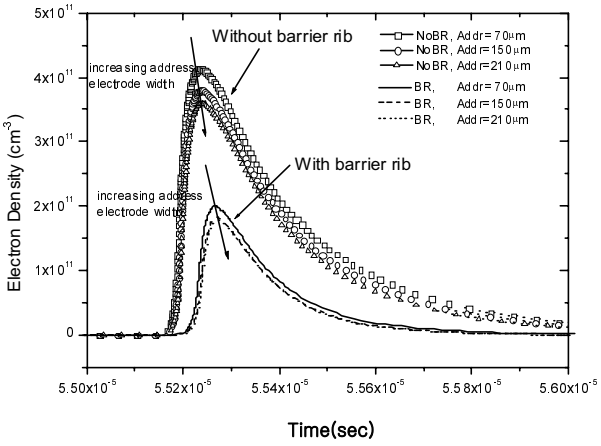

(a)

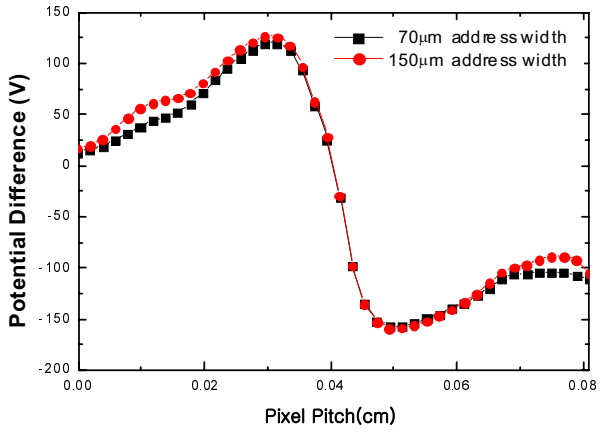

(b)

Fig. 1. (a) average electron densities for various address electrode width with and without barrier ribs (b) potential difference between the upper dielectric layer and the lower dielectric layer at z=90 μm.

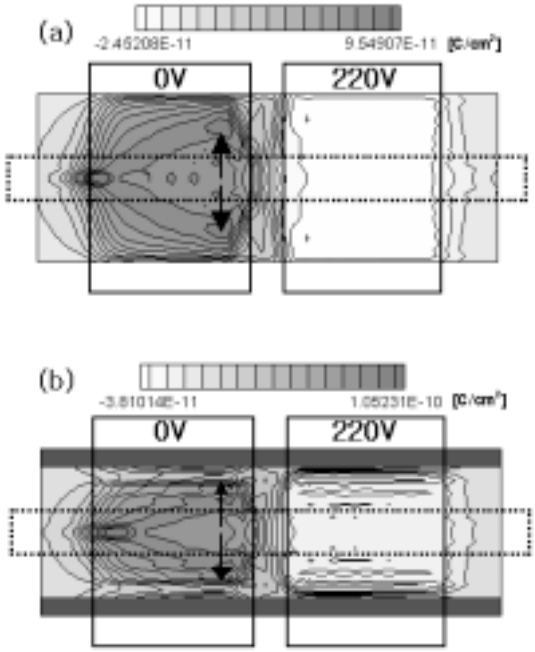

Fig. 2. Wall charge distribution on the upper dielectric layer: (a) without barrier ribs and (b) with barrier ribs. Bold solid line and dotted line show the sustain electrodes and the address electrode, respectively.

Fig. 2 shows wall charge distributions on upper dielectric layer in the case with and without barrier ribs. Wall charges are distributed over the whole sustain electrode as shown in Fig. 2(a). Electrons are uniformly accumulated on the dielectric layer, while ions are accumulated widely near the inner edge of the sustain electrodes and narrowly at the outer edge along the address electrode. More positive wall charges at off center of the left sustain electrode are obtained than at the center of the left sustain electrode along the address electrode due to drift and diffusion of ions produced during the discharge. The discharge ignites near the gap, and then the potential of the discharge region is increased due to accumulated ions. Because produced ions move along the surface toward regions where the potential is still low, the broader positive wall charge distribution near gap is obtained. Wall charge distributions accumulated at different positions of the barrier ribs are shown in Fig. 3 because the barrier ribs are considered with 3-D code. While maximum position of negative wall charge accumulated on the barrier ribs is located at 10 μm where is right under the upper dielectric layer, maximum positive wall charge is located near 30 μm under the upper dieletric layer. Because the address electrode acting as the cathode draws ions downward and pushes electrons upward, the maximum position of negative and positive wall charge accumulated on the barrier ribs is different.

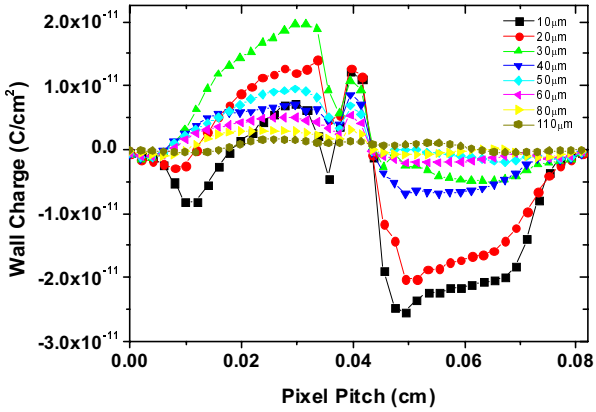

Fig. 3. Wall charge distribution accumulated on barrier ribs according to the location below the upper dielectric layer.

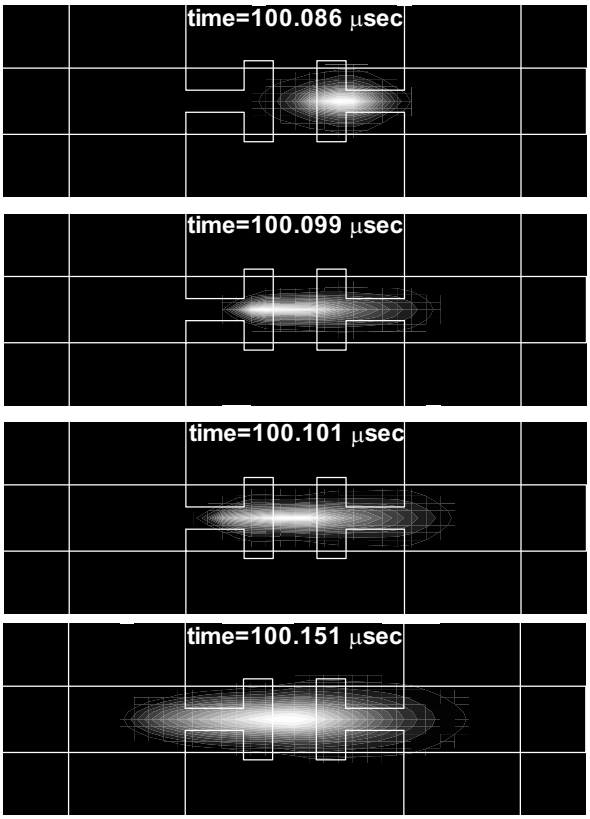

Fig. 4. Top views of electron density distribution at various times.

Fig. 4 shows the top views of electron density integrated along the height direction of the cell at various

times. Initially, the cell ignites with Vs=250 V and Va=125 V (Cell-ON mode) and after the cell reaches the a steady state (t=50 μs), the cell is sustained with Vs=220 V and Va=110 V during 50 μs (Sustain mode). Vs and 0 V are alternatively applied to sustain electrodes. After the discharge reaches a steady state in sustain mode, 220 V, 0 V, and 110 V are applied to the right, left, and address electrode, respectively. Then, the discharge ignites near the head portion of the right electrode at 100.086 μsec. After the discharge moves from the right head of T electrode to the left head of T electrode, it proceeds to ward the neck region of the left T electrode. After the electron density reaches its maximum value, it decreases and becomes wider along the perpendicular direction of the address electrode. Fig. 5(a) shows the wall charge distribution accumulated on the upper dielectric layer. Unlike the stripe case, the accumulated electron density is lower at the neck and the head of the electrode than at the outer edge. If the T electrode head thickness and neck width is narrow, the accumulated small wall charge near the ITO gap decreases potential difference between the two sustain electrodes in the next pulse thereby reguiring T electrode to have higher firing and sustain voltage. The wall charge distribution on the barrier rib along the cell height direction is shown in Fig. 5(b). Because the discharge intensity near ITO gap is weak and the electrodes are far away from the barrier ribs, a smaller amount of charge is accumulated at the center of the barrier rib unlike the stripe structure. Until 60μm below the upper dielectric layer, the polarity of wall charge is alternatively changed with the applied voltage.

Table. 1

Standard (Conventional electrode)
Width of ITO : 250 μm
Width of address : 75 μm
Barrier rib width : 30 μm (half of rib width)
Gas : Ne/Xe(4%), 500Torr
==========
T-shaped electrode
Reference (Ref.) : l=330, A=120, B=45, C=75
Case A : l=330, **A=180**, B=45, C=75
Case B : l=330, A=120, **B=60**, C=75
Case C : l=330, A=120, B=45, **C=100**
Case BC : l=330, A=120, **B=60**, **C=100**

We have simulated the effects of various parameters of T-shaped electrode by using 3-D code. Table. 1 and Fig. 6 show the simulation conditions and geometry. Cell size is 864 × 288 μm^2. In order to show the effect of T electrode reducing the power consumption, the simulation results of T electrode structure are compared with the results of conventional stripe structure with small ITO width (250 μm, namely Standard). Because power consumption is proportional to the sustain electrode area, when the sustain electrode length is increased, power consumption and UV production in

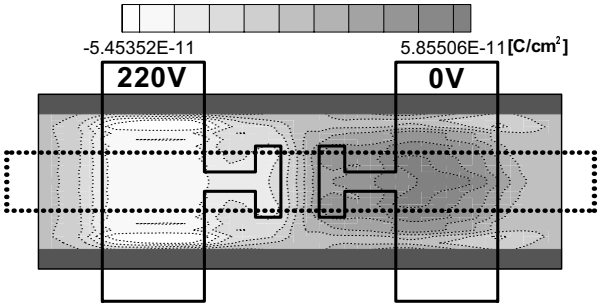

(a)

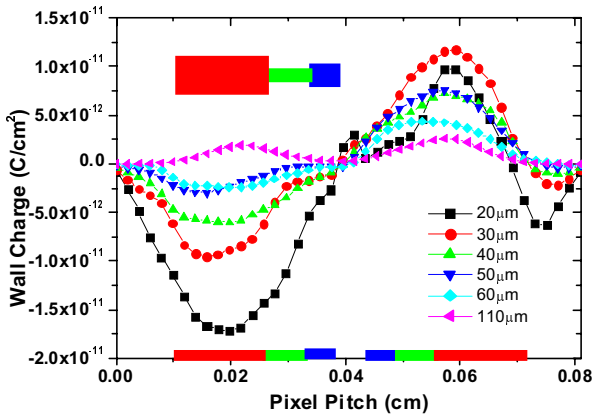

(b)

Fig. 5. Wall charge distribution of T electrode structure on (a) upper dielectric layer and (b) barrier rib according to the location below the upper dielectric layer. Bold solid line and dotted line show the sustain electrodes and the address electrode respectively.

discharge pulse are also increased. But because it is our objective to reduce power consumption so as to achieve high luminance efficiency, large electrode length cannot be used. T-shaped electrode structure has an electrode blank region that allows discharge current to be reduced. Thus,

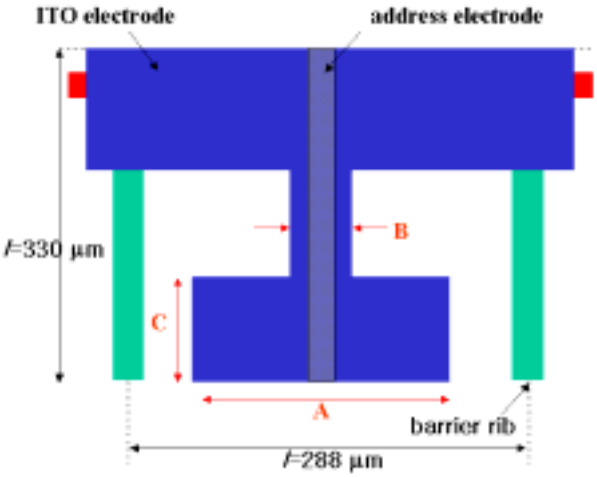

Fig. 6. Simulated T electrode structure.

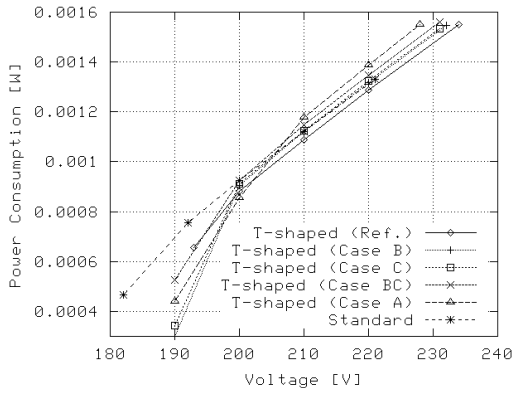

(a)

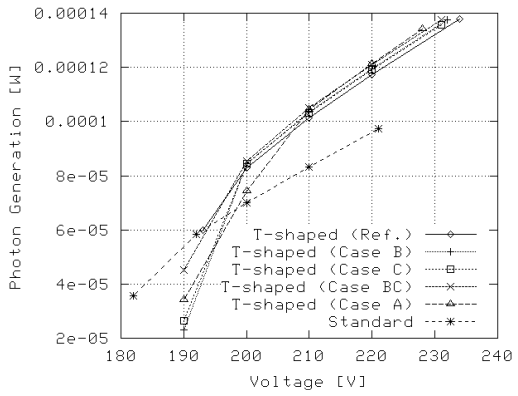

(b)

Fig. 7. (a) the simulated power consumption spent in heating electrons and ions (b) the power consumption spent in producing UV photons for various T electrode structures.

we use different electrode lengths for T electrode structure (l=330 μm) and standard structure (l=250 μm). We have varied width of T electrode head (Case A), neck of T electrode (Case B), height of T electrode (Case C), neck and height of T electrode (Case BC). Fig. 7(a) shows the simulation results for the power consumption. The breakdown voltage in T shaped electrode structure is increased due to the reduction in the electrode area near the gap and voltage margin shifts to higher voltage region than in stripe. Reference cell (Ref.) consumes less power than that of standard structure (Standard) because of small ITO area (15 % less). When each parameter is varied, the corresponding power consumptions are further increased than that in the case of reference cell (Ref.), as shown in Fig. 7(a). When the T electrode head width is increased (120 → 180 μm), the consumed power is increased and has its maximum value because the discharge region becomes wider. Fig. 7(b) shows the power consumed in producing UV photons in the discharge. Because T-shaped electrode structures have more UV photons and the reduced or a little increased power consumption than in the stripe structure, discharge efficiency ρ in T-shaped electrode is increased over 20 % higher than that of stripe structure. While plasma density is increased with the increase in T electrode head width, discharge efficiency is decreased due to fact that the loss of the plasma density toward barrier ribs is also increased. The height and neck in T electrode affect the breakdown voltage and discharge extension toward the outer edge of the sustain electrode, respectively. Because the height and neck of T electrode in our cell specification have width enough not to affect the breakdown voltage and discharge extension, reference cell with the smallest electrode area is highest in discharge efficiency.

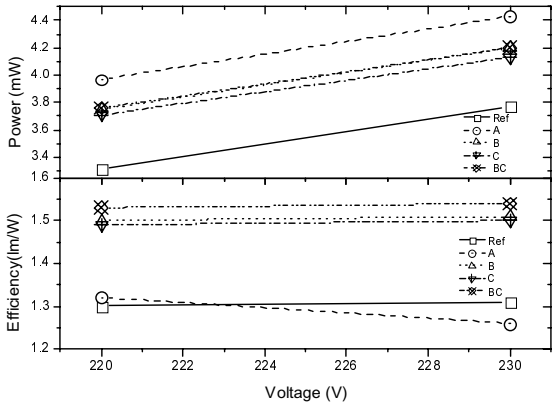

Fig. 8. Experimental results for the power consumption and luminance efficiency.

We have compared the simulation results with an experiment. Fig. 8 shows the experiment results for the power consumption and luminance efficiency. A 7.5 inch tests panel with the specification as shown in Table. 1 are made to verify the simulation results. Three panels are made for each case. Experimental results are measured with the voltage pulse of 5 khz and duty ratio 40 %. When the electrode shape and area are varied, the lowest power consumption for reference cell and the highest power consumption for "Case A" (increase of T electrode head width) are found to fall within 10 % good agreement with the simulation results. Such good agreement enables us to optimize the electrode structure using the simulation code. In the case of luminance efficiency, the results are found to be a little different from the simulation results. Although the simulation result shows that maximum efficiency is obtained in reference cell, "Case BC" has maximum efficiency in the experiment result. That is related to photons dynamics and the inclined barrier ribs. Although the simulation takes into consideration the production of UV photons, UV photons dynamics from their creation positions to phosphor layers is not considered. Thus, this simulation does not provide accurate results for luminance and the reflection effect of visible photons at the inclined barrier ribs with the test panels. The solution of Holstein's equation is needed to obtain accurate luminance quantities [9,10]. However, solving Holstein's equation is formidable in time and computer demanding. When the T electrode head width is increased, efficiency is also decreased as in simulation result.

4. Conclusions

We have investigated the effect of electrode shape using three-dimensional fluid code. The fact that the barrier ribs confine the discharge was ascertained from simulation results. The results of parameter variations showed that T electrode head width is a dominant factor in the power consumption and discharge efficiency. The dependences of power consumption on electrode shape and area are in good agreement with experiment.

References

[1] T. Nishio and K. Amemiya, Tech. Dig. of SID, 268 (1999).
[2] C. Punset, J.P. Boeuf, and L.C. Pitchford, J. Appl. Phys., **86**, 124 (1999).
[3] J. Meunier, Ph. Belenguer, and J.P. Boeuf, J. Appl. Phys., **78**, 731 (1995).
[4] Y. Hashimoto, Y. Seo, O. Toyoda, K. Betsui, T. Kosaka, and F. Namiki, Tech. Dig. of SID, 1328 (2001).
[5] C. K. Yoon, J. H. Yang, W. J. Cheong, K. C. Choi, and K. W. Whang, Proc. of The Seventh International Display Workshops, 627 (2000).
[6] H. C. Kim, S. S. Yang, S.W. Shin and J. K. Lee, J. Appl. Phys., **91**, 9513 (2002).
[7] H. C. Kim, S. S. Yang, and J. K. Lee, IEEE Trans. Plasma Sci., **30**, 188 (2002).
[8] P. L. G. Ventzek, R. J. Hoekstra, and M. J. Kushner, J. Vac. Sci. Technol. B**, 12**, 461 (1994).
[9] T. Holstein, Phys. Rev., **72**, 1212 (1947).
[10] T. Holstein, Phys. Rev., **83**, 1159 (1951).